Investigating strongly correlated electron systems with synchrotron X-ray diffraction at LNLS

Eduardo Granado[a,b,*]

[a]Instituto de Física "Gleb Wataghin", Unicamp 13083-970, Campinas-SP, Brazil
[b]Laboratório Nacional de Luz Síncrotron 13084-971, Campinas-SP, Brazil

Abstract

Recent X-ray diffraction measurements of strongly correlated electron systems performed at the Brazilian synchrotron light laboratory (LNLS) are described. These include the observation, by means of high-resolution powder diffraction, of small structural distortions likely associated with orbital ordering phenomena in transition-metal oxides, and magnetic diffraction of the intermetallic series $Gd_mM_nIn_{3m+2n}$ (M = Rh or Ir). These preliminary results illustrate the opportunities offered by the open facilities installed at the LNLS to investigations on strongly correlated systems.
© 2004 Elsevier B.V. All rights reserved.

PACS: 61.10.Nz; 75.25.+z; 75.40.−s

Keywords: Strongly correlated electron systems; Synchrotron X-ray diffraction; Intermetallic compounds; Magnetic materials

1. Introduction

Strongly correlated electron systems are presently one of the main frontiers of condensed matter physics, continuously generating phenomena of scientific and technological interest, such as high-temperature superconductivity in cuprates and colossal magnetoresistance in manganites. The high complexity of such systems has de-manded increasing sophistication of both theoretical and experimental approaches, and synchrotron light techniques have been systematically employed. With the advent of the Brazilian synchrotron light laboratory (LNLS), the first of its kind in the southern hemisphere, many of these techniques have become more easily accessible to the Latin American scientific community. Among the relevant experiments for strongly correlated systems already implemented at LNLS are: high-resolution X-ray powder diffraction, resonant magnetic diffraction on single crystals, and soft/hard X-ray absorption and dichroism in bulk or thin film samples.

*Instituto de Física "Gleb Wataghin", Unicamp, Cidade Universitária "Zeferino Vaz", Caixa Postal 6165, Campinas-SP 13083-970, Brazil. Fax: +55 19 3788 5427.

E-mail address: egranado@ifi.unicamp.br (E. Granado).

In this paper, I describe two experiments recently performed on strongly correlated systems, which might be taken as examples of the opportunities offered to this community by the open facilities installed at the LNLS. First of all, high-resolution synchrotron X-ray powder diffraction (S-XPD) measurements of the transition-metal oxide $La_{5/8}Ba_{3/8}Mn_{2/3}Fe_{1/3}O_3$ are presented. This compound shows small deviations with respect to an idealized cubic perovskite crystal structure. The temperature dependence of this lattice distortion, easily detected with synchrotron X-rays, are indicative of orbital ordering of Mn^{3+} $3d:e_g$ electrons in this chemically disordered system. Finally, resonant X-ray magnetic diffraction experiments on single crystals of the intermetallic series Gd_mMIn_{3m+2} (M = Rh or Ir, m = 1,2) are described. The magnetic structures at low temperatures, as well as the critical fluctuations in the ordered phases, are investigated and the relevance of these results to the physics of the heavy-fermion superconductivity shown by Ce-based members of this family is discussed.

2. Sample preparation and experimental setups

The powder sample of $La_{5/8}Ba_{3/8}Mn_{2/3}Fe_{1/3}O_3$ (LBMFO) was obtained from crystallites grown from high-temperature flux in a platinum crucible under dynamic growth regime [1]. The crystallites were ground in an agate mortar to reduce the grain sizes. The chemical composition was determined by X-ray fluorescence spectroscopy measurements, performed on the XRF beamline at LNLS. Gd_mMIn_{3m+2} (M = Rh or Ir, $m = 1, 2$) single crystals grown from the melt in In flux as described previously [2]. The crystal dimensions were larger than $2 \times 2\,mm^2$. The flat surfaces were finely polished to yield mosaic widths better than $\sim 0.1°$ full-width at half-maximum.

The high-resolution S-XPD measurements were performed on the D12A-XRD1 beamline, while magnetic X-ray diffraction measurements were performed on the D10A-XRD2 beamline [3], placed after dipolar sources at the LNLS. The Gd_mMIn_{3m+2} samples were mounted on the cold finger of a commercial closed-cycle He cryostat

with a cylindrical Be window, while LBMFO was mounted on a commercial cryofurnace, also with a cylindrical Be window. The cryostat was fixed onto the Eulerian cradle of a commercial $4 + 2$ circle diffractometer. The optics of both diffraction beamlines are similar. The energy of the incident photons is selected by a double-bounce Si(1 1 1) monochromator, with water-refrigeration in the first crystal, while the second crystal is bent for sagittal focusing. The beam is vertically focused or collimated by a bent Rh-coated mirror placed before the monochromator, which also provides filtering of high-energy photons (third- and higher-order harmonics). A vertically focused beam was used in our experiments, delivering, at 8 keV, a flux of $\sim 4 \times 10^{10}$ photons/s at 100 mA in a spot of $\sim 0.6\,mm$ (vertical) $\times\, 2.0\,mm$ (horizontal) at the sample, with an energy resolution better than $\sim 5\,eV$ (at 8 keV) in both beamlines. Our experiments were performed in the vertical scattering plane, i.e., perpendicular to the linear polarization of the incident photons. A solid state detector was used in the resonant magnetic diffraction experiments, while for high-resolution S-XPD a scintillation detector was placed after a Ge(1 1 1) analyzer crystal.

For LBMFO, complementary neutron powder diffraction measurements were performed on the BT-1 high-resolution powder diffractometer at NIST Center for Neutron Research (NCNR), using a monochromatic beam with $\lambda = 1.5402(1)\,\text{Å}$, produced by a Cu(3 1 1) monochromator. Collimations were 15′, 20′, and 7′ arc full-width at half-maximum before and after the monochromator, and before detectors, respectively.

3. Physical background, results, and discussion

3.1. High-resolution powder diffraction of $La_{5/8}Ba_{3/8}Mn_{2/3}Fe_{1/3}O_3$

A topic of current interest in the physics of transition-metal oxides is the identification of the most relevant mechanism of orbital ordering (OO) of 3d electrons [4]. A well-known system where the orbital physics plays a crucial role are the

manganites, where each Mn^{3+} ion shows an orbitally active $3d{:}e_g$ electron. While there is consensus that the OO patterns strongly influence the exchange interactions and by extension the magnetic order, the converse effect, i.e., the role of the exchange interaction in stabilizing the orbital order, is still a matter of debate. In fact, the electronic exchange between the degenerate orbitals is just a possible mechanism for OO in manganites. The alternative mechanism stems from the coupling of the degenerate orbitals to the lattice via electron–phonon interaction [4]. Experimentally, it is a difficult task to distinguish among the above possibilities. Substituting a fraction of the Mn ions by another transition metal such as Fe is a promising avenue, since the exchange interactions and strain fields are distinctly affected.

The magnetic, crystallographic, local atomic, and electronic properties of LBMFO were investigated by a wealth of techniques, including neutron scattering, synchrotron X-ray absorption and diffraction, resistivity, and DC- and AC magnetic susceptibility. The complete results will be published elsewhere [5]. Here I focus on the contribution of S-XPD to this work, complemented by neutron diffraction.

The crystal structure of LBMFO was Rietveld refined below 300 K using neutron data and an orthorhombic perovskite model with Imma symmetry, with the a and c lattice parameters constrained as equal. Thus, LBMFO shows a quasi-tetragonal perovskite structure. High-resolution S-XPD measurements were performed for LBMFO above room-temperature, using photons with wavelength $\lambda = 1.282$ Å. Unfortunately, the relatively large grain sizes that were obtained for the ground crystallites, even after extensive grinding ($> 20\,\mu m$) in conjunction with the small X-ray attenuation length at this wavelength ($< 10\,\mu m$) did not allow a satisfactory Rietveld analysis, due to poor grain averaging. Experiments at significant smaller wavelengths are not feasible on the bending magnet beamlines of LNLS, due to the relatively small critical energy of the emitted photons (2.08 keV). The temperature dependencies of the pseudo-tetragonal lattice parameters of LBMFO were then directly obtained from the

positions of the $(2\,0\,2)/(0\,4\,0)$ Bragg reflections. Fig. 1 shows such reflections at 300 K in comparison with neutron data at the same temperature, illustrating the usefulness in this case of the excellent angular and wavelength resolution obtained in this high-resolution S-XPD experiment. The temperature dependencies of the lattice parameters of LBMFO between 10 and 650 K are given in Fig. 2(a). Data are presented in terms of the "pseudo-cubic" lattice parameters, $a^* \equiv a/\sqrt{2} \approx c/\sqrt{2}$, and $b^* \equiv b/2$. The lattice parameters below and above room temperature were obtained using neutron and X-ray data, respectively, as explained above. In Fig. 2(a), a clear separation of b^* and a^* as the temperature decreases can be noticed. Fig. 2(b) shows the thermal evolution of $b^* - a^*$, indicating a change of behavior characteristic of an electronic phase transition at $T^* \approx 500$ K. It should be mentioned that the relatively large data dispersion in Fig. 2(a) above room temperature is not due to statistical errors in the fitting of $(2\,0\,2)/(0\,4\,0)$ Bragg reflections (Fig. 1), but rather a consequence of a slight compositional inhomogeneity between different grains, combined with
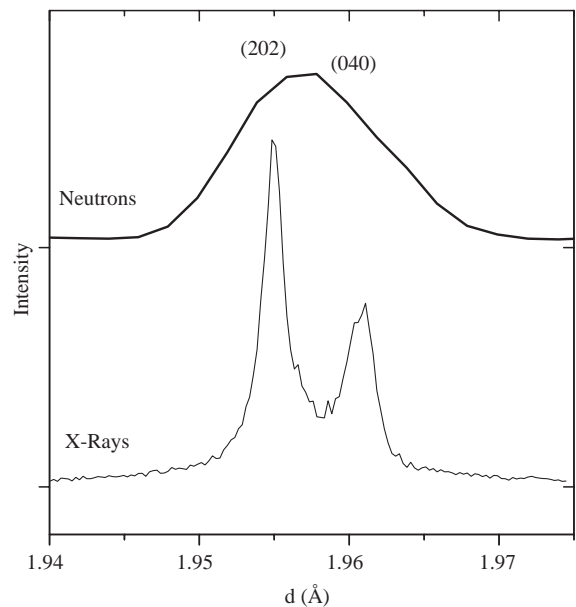

Fig. 1. Observed high-resolution neutron and synchrotron X-ray diffraction intensities of $La_{5/8}Ba_{3/8}Mn_{2/3}Fe_{1/3}O_3$ around the $(2\,0\,2)$ and $(0\,4\,0)$ Bragg reflections (orthorhombic notation), at 300 K.
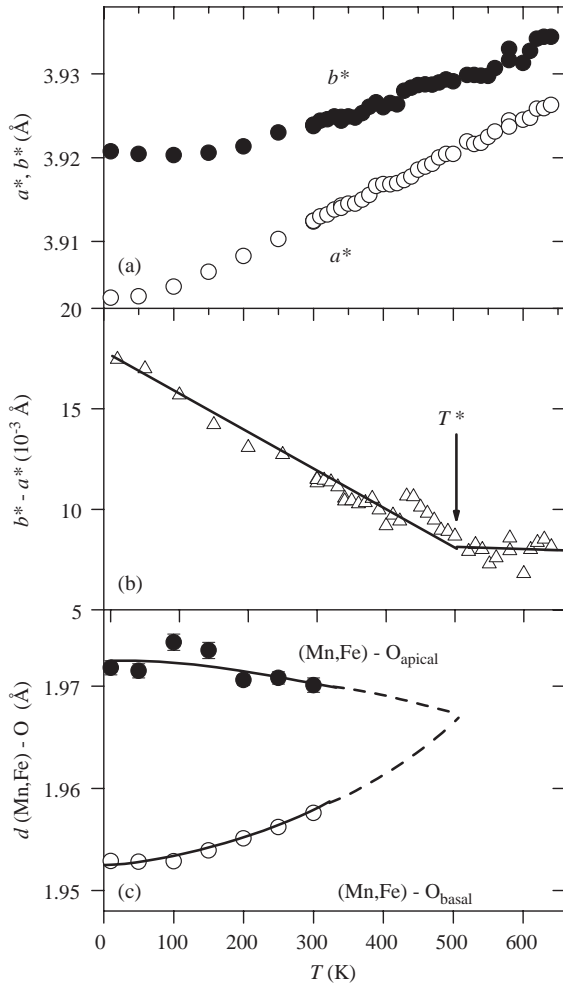
Fig. 2. Temperature-dependence of (a) "pseudo-cubic" lattice parameters $a^* \equiv a/\sqrt{2} \approx c/\sqrt{2}$ (empty symbols), and $b^* = b/2$ (filled symbols); (b) $b^* - a^*$ (c) (Mn,Fe)–O crystallographic distances along the b-direction (filled symbols), and ac-plane (open symbols) for $La_{5/8}Ba_{3/8}Mn_{2/3}Fe_{1/3}O_3$. Data below and above room temperature were obtained from the analysis of neutron and synchrotron X-ray powder diffraction data, respectively.

the poor grain averaging in our S-XPD experiments (see above).

A hint on the nature of the phase transition at T^* is obtained with the thermal evolution of the (Mn, Fe)–O bond distances below room temperature, obtained from neutron data (see, Fig. 2(c)). The average distortion of the $(Mn, Fe)O_6$ octahedra decreases with increasing T. Extrapolating this

behavior above room temperature (dashed lines in Fig. 2(c)), the transition to regular octahedra would occur at or near T^*. This indicates that the transition observed by S-XPD on the behavior of the lattice parameters at T^* is likely related to a long-range OO of 3d electrons.

X-ray absorption measurements performed at LNLS show single-valent high-spin Fe^{3+} (with no active orbital) and mixed-valence high-spin $Mn^{3+,4+}$, leading to a relatively low concentration of active orbitals per transition-metal site ($\sim 28\%$). Surprisingly, despite such dilute orbital concentration and the significant lattice and exchange disorder caused by substitution of $\frac{1}{3}$ of Mn ions by Fe^{3+}, long-range OO phenomena are still observed below a surprisingly high temperature, $T^* \approx 500\,K$. This observation is believed to severely constrain any plausible model of dilute OO in manganites.

3.2. Resonant magnetic X-ray diffraction of $Gd_m M In_{3m+2}$ (M=Rh or Ir, $m = 1, 2$)

The series of intermetallic compounds $R_n M_m In_{3n+2m}$ (R = rare earth; M = Co, Rh, or Ir) has recently attracted considerable interest due to the discovery of a new class of heavy-fermion superconductors for some compounds with R = Ce [6]. While the Cooper pairing mechanism remains unknown, most of the evidences point to anti-ferromagnetic spin fluctuations [7]. In order to fully understand the nature of the magnetic interactions in this system and their possible connection with the superconductivity found for R = Ce, it is necessary to investigate the evolution of the magnetic structure and fluctuations as a function of the rare earth ion R, as well as the dimensionality (n, m) [8]. The magnetism of Gd-based compounds is particularly relevant. This is because the $4f$ shell of this ion is half-filled with seven electrons, thus being spherically symmetric with null orbital magnetic moment. In this case, the crystal-field anisotropy, as well as any effect arising from the spin–orbit coupling, does not play a dominant role. Therefore, the magnetism shown by Gd-based compounds is a reliable signature of the dominant RKKY interactions and by extension of the Fermi surface of the system under

investigation. Since the neutron nuclear absorption cross-section of Gd is prohibitively high, alternative techniques must be employed to understand the microscopic magnetism of Gd-based compounds.

The magnetic structure and fluctuations of the layer $GdRhIn_5$ and bilayer Gd_2IrIn_8 tetragonal compounds were investigated by means of resonant X-ray diffraction [9]. Commensurate antiferromagnetic Bragg reflections were observed below $T_N = 40.4$ and 40.8 K for $GdRhIn_5$ and Gd_2IrIn_8, respectively. In both cases, the Gd spin arrangement is parallel along the tetragonal a-axis, and antiparallel along both the b- and the long c-axis. The magnetic structure of Gd_2IrIn_8 is illustrated in Fig. 3. The fact that the magnetic unit cell does not show the same tetragonal symmetry as the chemical one, being doubled
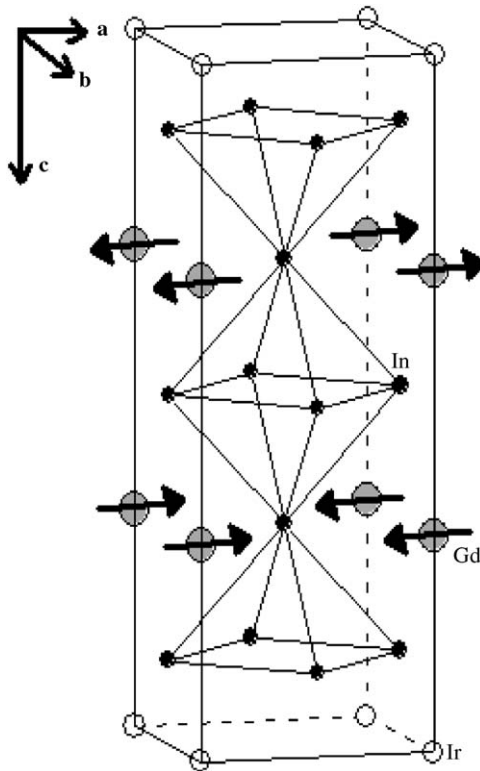

Fig. 3. Magnetic structure of Gd_2IrIn_8. The propagation vector is $\mathbf{k} = (\frac{1}{2}, 0, 0)$, and the spin directions are in the tetragonal ab plane.

along a particular tetragonal direction, is intriguing.

Remarkably, large dipolar enhancements of the magnetic Bragg reflections were observed at the Gd L_{II} and L_{III} edges for both samples (not shown, see Ref. [9]). Such characteristics suggest relatively high Gd:5d magnetic polarizations. Another interesting feature of the resonances is the magnetic diffraction anomalous fine structure (DAFS) observed above both studied edges and both samples (see Ref. [9]).

The temperature-dependencies of the magnetic order parameters close to the magnetic transitions are shown in Fig. 4 for both samples. No significant difference between the critical behaviors of $GdRhIn_5$ and Gd_2IrIn_8 in the ordered phase was observed. The critical parameter for the ordered magnetization is $\beta = 0.393(4)$ for Gd_2IrIn_8 and $\beta = 0.37(1)$ for $GdRhIn_5$, obtained from data taken above $\sim0.95\ T_N$. Such large values for β suggest that the magnetic fluctuations remain essentially three-dimensional in both layer and bilayer samples. It should be emphasized that, since crystal field or spin–orbit coupling effects do not play a determinant role for Gd-based compounds, such a property of the spin fluctuations is mostly a consequence of the exchange interactions. Thus, the exchange interactions remain three
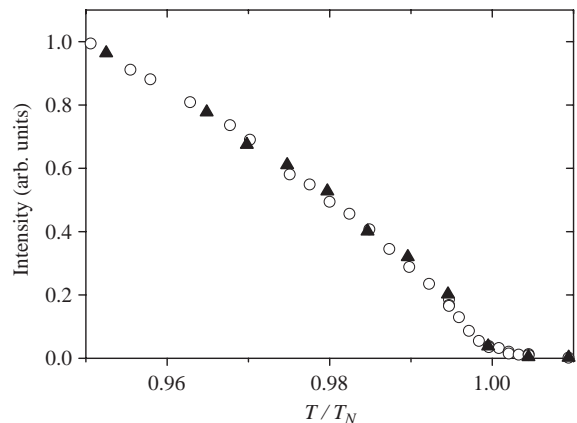

Fig. 4. Temperature dependence of the intensity of the Gd_2IrIn_8 $(\frac{1}{2}04)$ (open symbols) and $GdRhIn_5$ $(\frac{1}{2}0\frac{7}{2})$ (filled symbols) magnetic Bragg reflections at the vicinity of the Néel temperature T_N. The magnetic intensities are proportional to the square of the ordered magnetization.

dimensional for the layer $GdRhIn_5$ and bilayer Gd_2IrIn_8 despite the reduced dimensionality of the crystal structure. This is most likely a consequence of the long-range character of the RKKY exchange interactions, a conclusion presumably extensible to the other members of this family, in particular the Ce-based heavy-fermion superconductors [10].

The above results indicate that the strong dependence of the superconducting properties on the dimensionality of the crystal structure for the Ce-based compounds of this family takes place without a significant change of the dimensionality of the magnetic exchange interactions. Other electronic effects, such as crystal fields, must be invoked to understand the superconducting properties of this system [3,6,7].

4. Conclusions

In summary, small lattice distortions in the Fe-substituted doped manganite $La_{5/8}Ba_{3/8}Mn_{2/3}Fe_{1/3}O_3$ were studied by high-resolution synchrotron X-ray powder diffraction, evidencing a OO transition at a surprisingly high temperature, $T^* \approx 500$ K. Also, the magnetic structures and fluctuations of $GdRhIn_5$ and Gd_2IrIn_8 were successfully investigated by means of resonant X-ray diffraction at Gd L_{II} and L_{III} edges. In these compounds, the antiferromagnetic unit cells do not show the same tetragonal symmetry as the chemical ones, and the critical spin fluctuations in the ordered phases are demonstrated to be essentially three dimensional, despite the layered crystal structures. These selected examples illustrate the present capabilities of the diffraction beamlines at LNLS, as well as the large potential of synchrotron X-ray diffraction to the investigation of strongly correlated electron systems.

References

[1] S.N. Barilo, et al., J. Cryst. Growth 211 (2000) 480.
[2] H. Hegger, et al., Phys. Rev. Lett. 84 (2000) 4986.
[3] C. Giles, et al., J. Synchrotron Radiat. 10 (2003) 430.
[4] D.I. Khomskii, K.I. Kugel, Europhys. Lett. 55 (2001) 208.
[5] E. Granado, et al., to be published.
[6] C. Petrovic, et al., J. Phys.: Condens. Matter 13 (2001) L337;
C. Petrovic, et al., Europhys. Lett. 53 (2001) 254;
J.D. Thompson, et al., J. Magn. Magn. Mater. 226 (2001) 5.
[7] J.D. Thompson, et al., Physica B 329–333 (2003) 446.
[8] P.G. Pagliuso, et al., Phys. Rev. B 62 (2000) 12266;
W. Bao, et al., Phys. Rev. B 62 (2000) R14621;
W. Bao, et al., Phys. Rev. 63 (2001) 219901(E);
W. Bao, et al., Phys. Rev. 67 (2003) 099903(E);
W. Bao, et al., Phys. Rev. B 64 (2001) 020401;
M. Amara, et al., J. Magn. Magn. Mater. 130 (1994) 127;
M. Amara, et al., J. Magn. Magn. Mater. 131 (1994) 402;
S. Chang, et al., Phys. Rev. B 66 (2002) 132417.
[9] E. Granado, et al., Phys. Rev. B 69 (2004) 144411.
[10] W. Bao, et al., Phys. Rev. B 65 (2002) 100505.